

# Metallographic Preparation of Zn-21Al-2Cu Alloy for Analysis by Electron Backscatter Diffraction (EBSD)

M. G. Rodríguez-Hernández,<sup>1,\*</sup> E. E. Martínez-Flores,<sup>1</sup> G. Torres-Villaseñor,<sup>2</sup> and M. Dolores Escalera<sup>3</sup>

<sup>1</sup>Facultad de Ingeniería, Universidad Autónoma de San Luis Potosí, San Luis Potosí, San Luis Potosí, 78290, México

<sup>2</sup>Instituto de Investigaciones en Materiales, Universidad Nacional Autónoma de México, D. F., 04519, México

<sup>3</sup>Departamento de Ciencia e Ingeniería de Materiales, Universidad Rey Juan Carlos, Móstoles, Madrid, 28933, España

**Abstract:** Samples of Zn-21Al-2Cu alloy (Zinalco) that will be heavily deformed were prepared using five different manual mechanical metallographic methods. Samples were analyzed before tensile testing using the orientation imaging microscopy-electron backscatter diffraction (OIM-EBSD) technique. The effect of type and particle size during the final polishing stages for this material were studied in order to identify a method that produces a flat, damage free surface with a roughness of about 50 nm and clean from oxide layers, thereby producing diffraction patterns with high image quality (IQ) and adequate confidence indexes (CI). Our results show that final polishing with alumina and silica, as was previously suggested by other research groups for alloys that are difficult to prepare or alloys with low melting point, are not suitable for manual metallographic preparation of this alloy. Indexes of IQ and CI can be used to evaluate methods of metallographic preparation of samples studied using the OIM-EBSD technique.

**Key words:** electron backscatter diffraction, orientation imaging microscopy, specimen preparation, Zn-Al alloy, atomic force microscope

## INTRODUCTION

The biphasic alloy Zn-21Al-2Cu (trade name Zinalco) has a low melting point (421–481°C). This alloy can be processed by casting, rolling, or extrusion (Negrete et al., 1995, 1999) and under certain conditions of temperature, strain rate, and microstructure is deformed superplastically, elongating more than 500% with very low stress. This property is relevant because this alloy can be manipulated into formed parts with complex geometries using thermoforming techniques, thereby providing energy and machinery savings that are significant at an industrial level. Some applications for this alloy include gas valves, keys, window profiles, auto parts, and making of car bodies without soldering. We are interested in studying microstructural changes of this alloy during superplastic deformation in tension, because this material is not deformed homogeneously as described in established mechanisms for other biphasic alloys superplastically deformed. The experimental approach is orientation imaging microscopy-electron backscatter diffraction (OIM-EBSD) in which a scanning electron microscope is used. An electron beam strikes the sample, which is tilted 70° from the horizontal axis. A phosphor screen is placed near the sample in order to detect diffracted backscattered electrons. The obtained electron backscatter patterns (EBSPs) provide crystallographic information for each point that is touched by the incident beam. To ensure the reliability of indexing, these patterns

must be well-defined. Sharpness of the EBSPs depends on the contrast between the bands and can be evaluated using two parameters: the image quality (IQ) index and the confidence index (CI), (TSL-EDAX, 2001; Wright & Nowell, 2006). The Kikuchi patterns can be affected by distortions in the crystal lattice near the surface (e.g., twins, dislocations, or vacancies), along with the topography of surface, contaminants, surface dirt, oxide layers, and deformations introduced on the surface during metallographic preparation of the sample (Nowell et al., 2005; Wynn & Boehlert, 2005; Schwartz et al., 2009; Vander Voort, 2011a). Even though the OIM-EBSD technique is increasingly being used as a standard tool for micro-characterization, there are still some adjustments required for this technique to be useful in studying materials that are heavily deformed, especially regarding metallographic techniques for sample preparation that allow acquisition of EBSPs with high quality, and to determine fine substructures, crystallographic orientation, and grain size of heavily deformed materials (Waryoba & Kalu, 2003). Metallographic preparation methods cause changes in sample topography and may introduce damage to the surface of the sample. The topography and damaged surface may interfere with trajectories of the backscattered electrons when they emerge on the surface, thereby decreasing the amount of electrons that impact the phosphor screen and thus, diminishing the EBSPs quality (Nowell et al., 2005; Wynn & Boehlert, 2005).

Wynn and Boehlert (2005) studied the association between the IQ of Kikuchi patterns and roughness of the sample surface; they concluded that sharp diffraction patterns are obtained with samples that have a roughness of

about 50 nm and below this value, sharpness of the Kikuchi patterns is mainly influenced by the degree of damage on the surface caused during metallographic preparation. Some research groups have claimed that a flat and damage free surface (one that is free from roughness), can only be achieved using electropolishing techniques; however, it has been shown (Waryoba & Kalu, 2003; Nowell et al., 2005; Vander Voort, 2011a, 2011b; Witt & Nowell, 2011) that diffraction patterns with excellent quality can also be obtained when mechanical polishing is used. It has been reported that some special mechanical polishing methods can be used to obtain well-polished deformation free surfaces (Vander Voort, 2011a, 2011b), but there are still adjustments to be made because these methods do not work well for certain materials such as magnesium and titanium alloys, or heavily deformed alloys (Waryoba & Kalu, 2003; Witt & Nowell, 2011). Moreover, in Zn-Al alloys, the zinc-rich phase is more reactive when fine grains are formed, so it is not advisable to use electropolishing to obtain a flat surface that is oxide-free (Guerrero et al., 2002).

Some Zn-Al-based alloys have been studied using EBSD. In these works the OIM-EBSD technique was used to determine phases that are present in the alloy (Zhu et al., 2001) as well as a complementary technique in the study of microstructural changes on as casting or extruded and subsequently solubilized Zn-Al alloys (Zhu et al., 2001, 2003). In these studies mechanical polishing with diamond pastes of 6 and 4  $\mu\text{m}$  were made and EBSPs were obtained, however, in the discussion of the phase maps, the authors indicated that there were large areas that could not be indexed. Therefore, this polishing method was not suitable for study of superplastically deformed Zinalco. In order to study the superplastic deformation mechanism of the Zinalco alloy, tensile samples should be properly prepared before subjecting them to the superplastic deformation process, because changes in the microstructure after superplastic deformation will be studied and an additional metallographic preparation will not be made. The aim of this study was to determine the appropriate conditions for manual mechanical polishing of

Zn-21Al-2Cu tensile samples that will be used to study the superplastic deformation mechanisms that will be reported in a subsequent paper.

## MATERIALS AND METHODS

The alloy was prepared from pure elements and cast in a suitable composition. Moreover, it was solidified by continuous casting. A solidified rod was subjected to successive processes of inverse extrusion at 290°C and hot rolling at 240°C until a 48% thickness reduction was achieved. This thermo-mechanical treatment helped to break the dendritic microstructure obtained after the solidification process. Tension specimens were cut from rolling sheets, and these samples were solubilized by treating them for 1 h at 350°C, followed by a water quench at 15°C. The resulting biphasic fine-grained microstructure was stabilized by annealing at 250°C for 20 min (Negrete et al., 1995; Ramos Azpeitia et al., 2012). After all stages of the thermo-mechanical processing were completed, the alloy had a fine-grained microstructure as shown in Figure 1a. The linear intercept method was used to determine grain size, which was  $\leq 1 \mu\text{m}$ . The Brinell hardness under these conditions was 75. This kind of microstructure is necessary for superplastic deformation of this alloy and is formed mainly by two different solid solutions that are  $\alpha$  and  $\eta$  phases. The  $\alpha$ -phase is an aluminum-rich solid solution (dark grains) while the  $\eta$ -phase is a solid solution rich in zinc (light grains). Note that the microstructure that is shown in Figure 1a corresponds to that of a sample with a mirror finish and no etching. Determining the grain boundaries by etching was not possible due to the reactivity of the zinc-rich phase. The microstructure, after etching (Fig. 1b), shows that the zinc-rich phase reacted with the etching solution, resulting in a microstructure mainly composed of the aluminum-rich phase (dark areas) with some regions of zinc oxide (bright areas).

Samples were cut in the form of tensile specimens to be used to assess microstructure changes caused by the superplastic deformation of this alloy. Tensile specimens were cut parallel to the rolling direction in the following

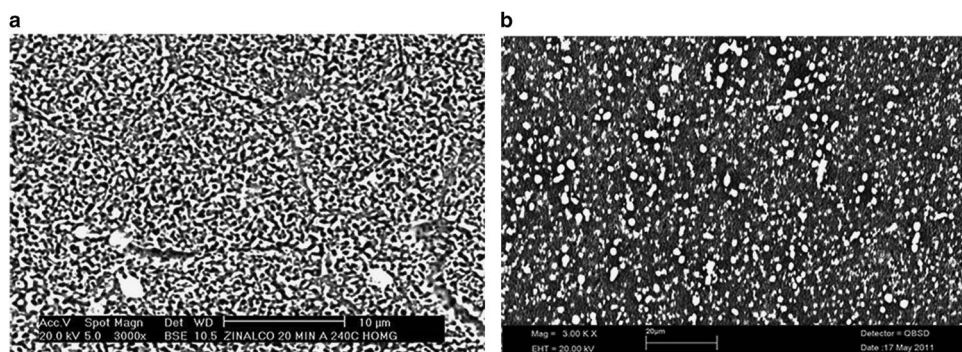


**Figure 1.** The microstructure of Zn-21Al-2Cu alloy after thermo-mechanical treatments. **a:** Sample with mirror finish and no etching. The dark phase corresponds to an aluminum-rich solid solution phase called  $\alpha$ , and the clear phase is a zinc-rich solid solution phase called  $\eta$ . **b:** Etched sample. The bright phase is zinc oxide, and the dark phase corresponds to the aluminum-rich solid solution.

**Table 1.** Particle Size of Abrasive Used and Time of Sanding/Polishing for the Metallographic Preparation of Zn-21Al-2Cu Alloy.

Method	Al <sub>2</sub> O <sub>3</sub> (μm)		Diamond (μm)	Al <sub>2</sub> O <sub>3</sub> (μm)	SiO <sub>2</sub> (μm)
	5–1	0.3	0.1	0.05	0.04
1	5 min	–	–	–	–
2	5 min	5 min	–	–	–
3	5 min	5 min	1 min	–	–
4	5 min	5 min	1 min	1 h	–
5	5 min	5 min	1 min	1 h	1 h

**Table 2.** Conditions for Each Metallographic Preparation Step Used for Zn-21Al-2Cu Alloy.

	Abrasive/size	Speed (rpm)	Time	Rotation direction	Dispense
Grind	1,000 mesh SiC 1,500 mesh SiC 2,000 mesh SiC 4,000 mesh SiC	200	10 s	Contra	Continuous water
Rough polish	5–1 μm Al <sub>2</sub> O <sub>3</sub> 0.3 μm Al <sub>2</sub> O <sub>3</sub> 0.1 μm diamond	0 0 0	5 min 5 min 1 min	– – –	Distilled water every 30 s Distilled water every 30 s Ethylene glycol every 120 s
Final polish	0.05 μm Al <sub>2</sub> O <sub>3</sub> 0.04 μm SiO <sub>2</sub>	– –	1 h 1 h	– –	Distilled water every 30 s on a vibratory polisher Distilled water and SiO <sub>2</sub> every 30 s on a vibratory polisher

dimensions: 6.35 mm gauge length, 2 mm radius of curvature, 5.0 mm wide, and 2.54 mm thickness. After rolling, a flat surface with good finishing was obtained, so the samples were sequentially sanded with emery paper mesh sizes of 1,000, 1,500, 2,000, and 4,000. A new abrasive paper was used in each step because the effectiveness of the abrasive decreases with use.

Five metallographic preparation methods for this alloy were evaluated. Two of them, i.e., Methods 4 and 5, used abrasives that were previously reported (Nowell et al., 2005; Vander Voort, 2011a, 2011b). The effect of particle size for each type of abrasive on sharpness of diffraction patterns was studied, and the details are reported in Table 1. For each method, the abrasive particle size decreased progressively in each stage until a size of 0.04 μm was reached. Method 1 consisted of a rough polish using alumina (i.e., 1–5 μm in size) on a MicroCloth (Buehler). Method 2 contained an added polishing step with Buehler's alumina (0.3 μm) on the same type of cloth. Method 3 used the aforementioned steps, followed by polishing with a Leco diamond paste of 0.1 μm applied with a Struers DP-NAP cloth. The coarse polishing with alumina and diamond paste (Methods 1–3) was performed manually; i.e., the sample was gently slid across the polishing cloth, while the polisher disk was held steady to prevent material dragging and to minimize damage caused during the metallographic preparation. The final polishing steps were done using a Vibromet polisher (Buehler) for 1 h. At this stage, the following abrasives were used: Al<sub>2</sub>O<sub>3</sub> of 0.05 μm, followed by OP-S colloidal silica of 0.04 μm (Struers); in each case, MicroCloth (Buehler) was

used. Deionized water was added 15 s before the final polishing ended with colloidal silica to clean the remaining abrasive from the cloth. At the end of the polishing the sample was immediately wiped with tap water and ethanol to prevent the silica from crystallizing on the sample surface and to eliminate silica particles which may be weakly bound to the sample surface (Zipperian, 2011). To prevent abrasive particles from becoming embedded on the sample surface after each grinding and polishing step, the sample was ultrasonically washed with ethanol for 5 min. All conditions used for sample preparation are summarized in Table 2.

Kikuchi patterns were obtained using a charge-coupled device camera and a DigiView III XM4 Pegasus detector with a resolution of 348 × 260 pixels in a SEM230 Nova Nano (FEG-SEM, FEI Company, Hillsboro, Oregon, USA). The following conditions were used: an accelerating voltage of 20 kV, a beam current of 6 nA, and a working distance of 15 mm. The sample was tilted 70° from the horizontal axis and was dynamically focused. Grain maps were created using data analysis and the processing software OIM TSL 5.13. According to Humphreys (1999), the minimum number of points required for the analysis of grain size is 20,000. Considering this, sweeps of 4 × 4 μm areas were conducted using a hexagonal measurement grid with a step size of 0.025 μm, ultimately resulting in ~29,508 collected points at a speed of 80 patterns per second with an acquisition time of 48 min. Post-processing of the data was accomplished using a level 0 grain dilation clean-up; this adjustment only acts on points that do not belong to any grain because they were not properly

indexed (i.e., white dots). The orientation of each white point was assigned according to the orientation of the closest point with the highest CI value. The CI value and the IQ index that were obtained after data processing with the TSL OIM 5.13 software were used as parameters to evaluate each preparation method (TSL-EDAX, 2001; Wynick & Boehlert, 2005).

As previously mentioned, manual mechanical polishing may result in surface damage that can decrease the sharpness of Kikuchi patterns. Therefore, we determined whether a flat and damage free surface suitable for characterization of this alloy was achieved after polishing using an EBSD technique. This was determined by measuring the mean square roughness ( $R_q$ ) using an atomic force microscope, i.e., the Nanosurf EasyScan. A  $20 \times 20 \mu\text{m}$  area was analyzed in contact mode with a maximum scanning speed of 1,800 points per second.

## RESULTS AND DISCUSSION

Specimens that are machined after lamination have flat surfaces that do not require coarse grinding. Cutting or sectioning of the sample is an aggressive process that produces massive damage. After the lamination process, it was not necessary to cut the sample so a grinding coarse was not required, which is usually done to remove the damaged surface by cutting it (Vander Voort, 2011a). The abrasive thickness used during grinding determined the depth of damage introduced during sample preparation. If the abrasive used was too thick, the damage induced was not eliminated in the following steps. Sanding was started with 1,000 mesh SiC sandpaper to prevent deep damage to the surface that could not be removed in the following steps. For zinc alloys, alumina was recommended (Vander Voort, 1999) for both coarse and final polishing, because this abrasive is able to remove more material. To remove roughness without causing excessive damage, Vander Voort (2011a) also recommended performing a final polish using  $0.05 \mu\text{m}$  alumina or colloidal silica in a vibratory polisher for 1–2 h.

Methods 1 and 2 implemented the suggestions made in the work by Vander Voort and collaborators (Vander Voort, 2011a). When these methods were used to prepare specimens of Zn-21Al-2Cu alloy, a slightly opaque sample surface was observed after polishing because an oxide film characteristic of this alloy was formed (Torres-Villaseñor et al., 1984); therefore, using this film would affect the sharpness of the Kikuchi patterns.

In Method 3, it was proposed that the oxide layer that formed when using alumina in Methods 1 and 2 could be reduced. Method 3 involves an additional polishing step using a diamond paste of 0.1 microns and ethylene glycol as a dispersant to reduce oxidation. In this last step, the sample was polished for 1 min without applying pressure to avoid scratching, minimizing the damage on the surface. This additional step was added in an attempt to obtain sharper EBSPs.

In Method 4, a final polishing stage using  $0.05 \mu\text{m}$   $\text{Al}_2\text{O}_3$  in a vibratory polisher was added as recommended by Vander Voort (2011a) to improve the sharpness of the Kikuchi patterns for low melting point metal alloys. However, we observed

that the sample surface turned gray and did not have an even tone when this final polishing stage was added. An energy dispersive X-ray analysis indicated the presence of zinc oxide probably due to the use of water as the dispersant. This finding is consistent with previous reports (Hernandez et al., 2003).

In Method 5, an additional step in the final polishing procedure was added; this step was also suggested by Vander Voort (2011a). In this step, samples were polished with colloidal silica for 1 h in a Vibromet polisher. However, after polishing the samples for 10 min, we found that the sample surface was opaque. This was probably because there's a reaction caused by the pH value (between 9 and 10) of the silicon dioxide suspension that was in contact with the sample surface. (Gaishun et al., 2002). This pH value may promote formation of hydroxides on the sample surface, which can interfere with the ability to obtain sharp Kikuchi patterns.

To properly polish this alloy, new cloths must be used for each step of the experimental work. Cloths should be washed constantly to remove material that gets caught in them, preferably after each use with a polished sample. To avoid causing damage to the sample surface. The polishing steps involving alumina and diamond paste are described in Table 2 and were conducted with a stable, non-moving polishing disk because we found that drag material was produced even when using the minimum load and speed, especially with the finest abrasives. For the polishing step, the sample should be manually slid across the surface without pushing it.

An atomic force microscope was used to determine the roughness of the samples prepared with each of the methods proposed in Table 1. Figure 1a shows a representative image of the topography that was observed in the samples after polishing them using Method 3. The roughness profile that was measured over the same area is shown in Figure 1b. We obtained an average roughness of 12.3 nm. The obtained roughness results for this method are shown in Figure 2b.

The roughness values ( $R_q$ ) was determined in order to evaluate each of the tested methods and the results are shown in Figure 3. The  $R_q$  for the sample prepared by Method 1 was 125.6 nm. This large roughness value was caused by the wide range of particle size for the abrasive surface, i.e., 1–5  $\mu\text{m}$ . The large particles in this abrasive substance produced grooves that were caused by dragging material from the surface, so this step was part of the rough polish of the material. The  $R_q$  values for samples prepared by Methods 2 and 3 were 17.2 and 12.1 nm, respectively; we observed a significant decrease in roughness in the samples prepared by Methods 2 and 3 as compared with the roughness of the sample prepared with Method 1. This demonstrates the effect of particle size reduction in the additional polishing steps included in Methods 2 and 3. A reduction in abrasive particle size resulted in a flatter surface for samples prepared by Methods 2 and 3 as compared with that of Method 1. The  $R_q$  value of the sample prepared by Method 3 is slightly smaller than that of Method 2. Methods 4 and 5 added additional final polishing stages with very fine abrasives. However, we observed a significant increase in the roughness of samples

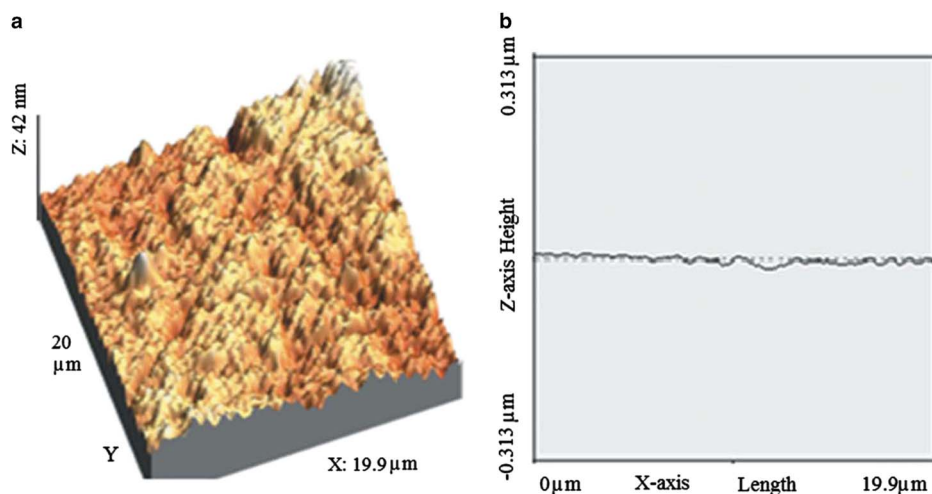


**Figure 2.** **a:** Atomic force microscope (AFM) image of Zn-21Al-2Cu mechanically polished using Method 3. **b:** Roughness profile of same sample.

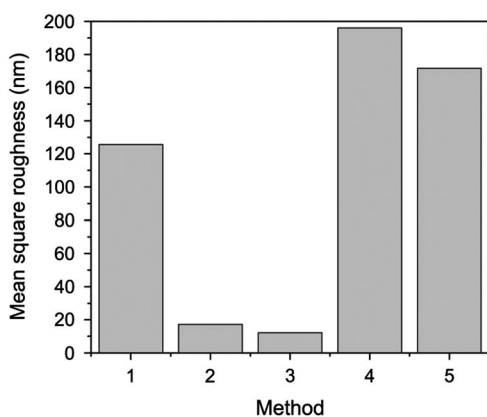


**Figure 3.** Mean square roughness ( $R_q$ ) for each of the methods listed in Table 1.

prepared by these methods as compared to that of the first three. The  $R_q$  value was 196 nm for the sample prepared by Method 4 due to formation of an irregular oxide layer caused by the addition of water as a dispersant when 0.05 m alumina was used. After using colloidal silica in Method 5, the roughness decreased slightly; i.e., the  $R_q$  value was 171 nm. However, the pH of the polishing solution created an opaque surface, probably due to the formation of hydroxides. Ultimately, if the topography was the only factor that could affect the sharpness of a Kikuchi pattern obtained with an EBSD technique, then the most suitable preparation Methods would be 2 and 3.

Kikuchi patterns for samples that were prepared using each of the five proposed methods were obtained via the OIM-EBSD technique. The patterns were indexed using crystallographic data from the solid solutions that were present in the alloy; this information was previously obtained from the collection software database. Grain maps were created in order to obtain average values for the CI and IQ index. These parameters were chosen to evaluate the preparation methods that are proposed in this paper. The IQ

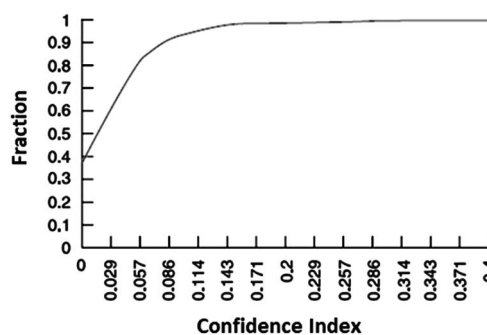


**Figure 4.** Fraction of points correctly indexed as a function of the confidence index of Kikuchi patterns in the fcc materials (TSL-EDAX, 2001).

index values were normalized using the highest value obtained. The CI can be related to the correctly indexed patterns in the fcc materials. According to the graph shown in Figure 4, CI values  $\geq 0.08$  indicate that  $\sim 90\%$  of the patterns have been indexed correctly; this means that the microstructure reconstruction is complete (TSL-EDAX, 2001).

The normalized IQ values and percent of appropriately indexed patterns for samples prepared via the five methods under investigation are presented in Figure 5. To evaluate the effect of the preparation methods on sharpness of the Kikuchi patterns, some images were captured and are shown in Figure 6. With the obtained data, grain maps were constructed to show the degree of microstructure reconstruction depending on the preparation method. These maps are shown in Figure 7.

Normalized IQ values for samples prepared by Methods 1 and 2 were about 83% in both cases. If we analyze the Kikuchi patterns obtained for these samples (Figs. 4a, 4b, respectively), we can see that both patterns are very poor in terms of sharpness. In these cases, the CI values were between 0.03 and 0.04, which indicates that only 60–70% of the diffraction patterns were indexed correctly (Fig. 5). These IQ and CI

values indicate that a considerable number of patterns could not be indexed and thus appear as white dots on the map of grains (Figs. 5a, 5b, respectively). The microstructure cannot be reconstructed completely with these preparation methods. As shown in Figure 5, a normalized IQ value of 100% was obtained for the sample prepared using Method 3.

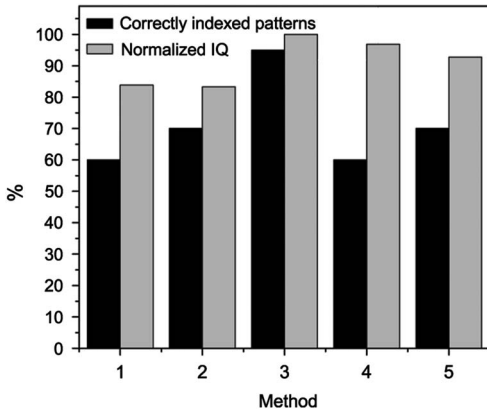


**Figure 5.** Normalized image quality (IQ) values and percentage of correctly indexed patterns obtained for polished samples using each of the five studied methods.

This indicates that the obtained Kikuchi patterns had good sharpness (Fig. 6c). In this case, the obtained CI value was 0.09, which indicates that ~95% of the patterns were correctly indexed. The grain map in Figure 7c shows a minimal number of white spots. The results obtained with Method 3 were better than the ones obtained with Methods 1 and 2. This is because Method 3 allowed removal of the oxide layer formed in the previous methods. Also, Method 3 minimized the load and polishing time and performing this step with a fixed disk minimized damage on the surface of the sample.

Final polishing stages that were added in Methods 4 and 5 caused a decrease in the normalized IQ values to about 95% for both methods. The diffraction patterns obtained from samples prepared by these methods (Figs. 6d, 6e, respectively) show a decrease in sharpness as compared with the pattern obtained from the sample prepared with Method 3 (Fig. 6c). This decrease in sharpness is attributed to the formation of an oxide layer in Method 4 and the formation of hydroxides in Method 5. CI values obtained for samples prepared with Methods 4 and 5 were 0.03 and 0.04, respectively (Fig. 5). This indicates that only 60–70% of the patterns were indexed properly. Figures 7d and 7e show a significant number of white points that could not be properly indexed; consequently, a complete reconstruction of the

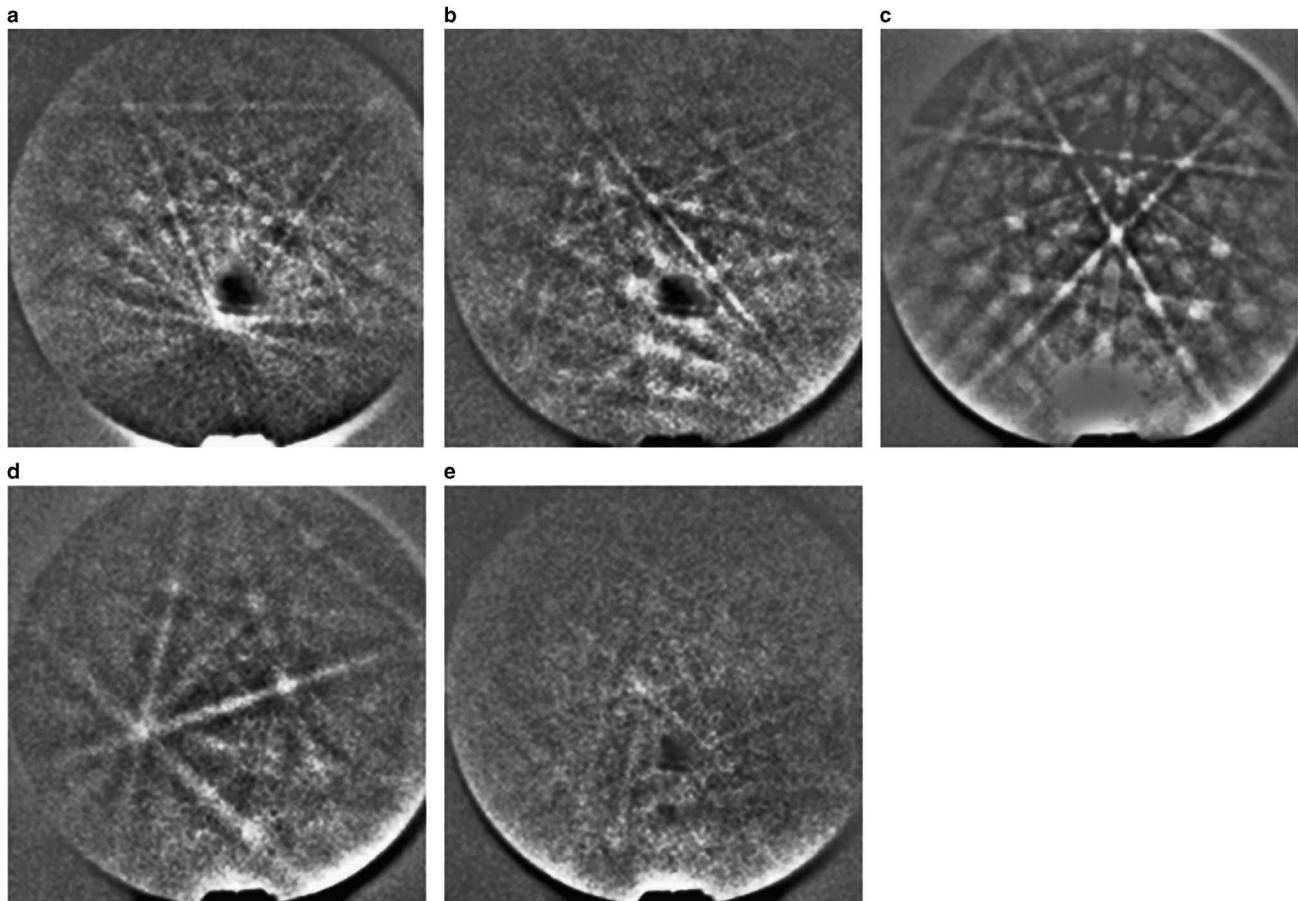


**Figure 6.** Kikuchi patterns. **a:**  $\eta$  phase, using Method 1; **(b)**  $\alpha$  phase, using Method 2; **(c)**  $\eta$  phase, using Method 3; **(d)**  $\alpha$  phase, using Method 4, and **(e)**  $\eta$  phase using Method 5 as described in Table 1.

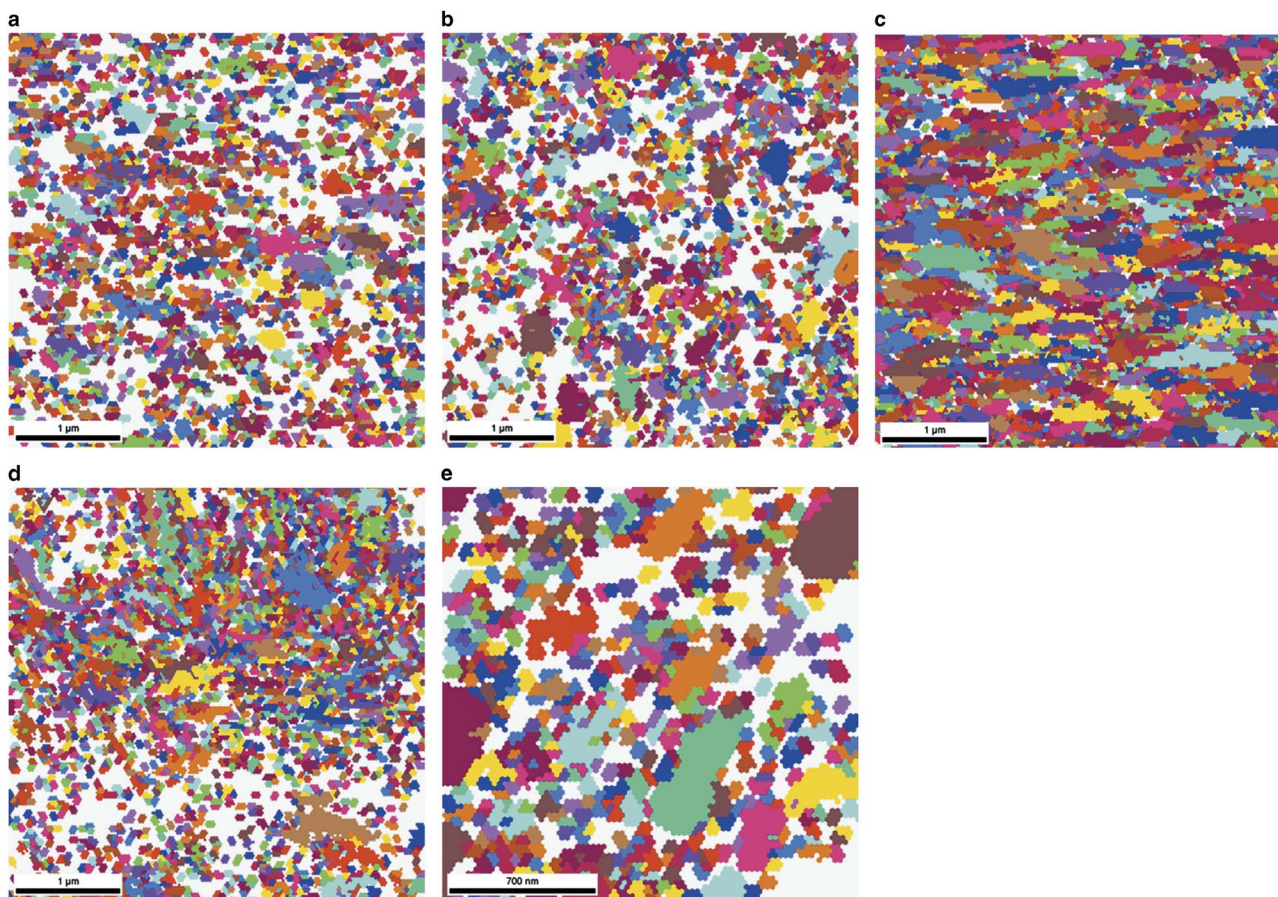


**Figure 7.** Grains maps of samples prepared with (a) Method 1, (b) Method 2, (c) Method 3, (d) Method 4, and (e) Method 5.

microstructure could not be done. Based on these results, we can conclude that the final polishing step in a metallographic preparation procedure is not recommended for this alloy due to the poor diffraction patterns in terms of sharpness and the incomplete microstructure rebuild obtained from OIM-EBSD on samples that were prepared with the inclusion of this step.

## CONCLUSIONS

This study established a method for the manual mechanical polishing of Zn-21Al-2Cu alloy. Using this preferred method, high-quality Kikuchi patterns were obtained, and a complete reconstruction of the microstructure via the OIM-EBSD technique was achieved. The preferred method consists of using 1–5  $\mu\text{m}$  alumina, followed by 0.3  $\mu\text{m}$  alumina and finally 0.01  $\mu\text{m}$  diamond paste (i.e., Method 3). With this method, a flat surface free of rust with an average roughness of 12.7 nm was obtained.

For this alloy, final polishing with alumina on a vibratory polisher is not recommended due to formation of a thin oxide layer on the sample surface. This oxide layer increases roughness, thus diminishing the CI and IQ values. Moreover, the use of a colloidal silica suspension is not recommended, because the high pH value of the aqueous solution will

produce an opaque surface on the sample. This may be due to formation of hydroxides on the surface that will affect sharpness of the Kikuchi patterns.

A direct correlation between roughness of the surface and the obtained IQ and CI values using the OIM-EBSD technique was observed. Therefore, both parameters can be used to evaluate the method used for metallographic preparation of samples.

## ACKNOWLEDGMENTS

The authors acknowledge receipt of financial aid through Project C10-FAI-05.04.67. They are grateful to Ms. Rocío Alfaro Guevara and Dr. Salvador Palomares Sanchez for their technical assistance in the use of atomic force microscopy.

## REFERENCES

- GAISHUN, V.E., TULENKOVA, O.I., MELNICHENKO, I.M., BARYSHNIN, S.A., POTAPENOK, Y.A., XLEBOKAZOV, A.P. & STREK, W. (2002). Preparation and properties of colloidal nanosize silica dioxide for polishing of monocrystalline silicon wafers. Available at: [http://materialscience.pwr.wroc.pl/bi/vol20no2/articles/ms\\_2001\\_013.pdf](http://materialscience.pwr.wroc.pl/bi/vol20no2/articles/ms_2001_013.pdf).

- GUERRERO, R., FARIAS, M.H. & COTA-ARAIZA, L. (2002). Increase in corrosion resistance of Zn-22Al-2Cu alloy by depositing an Y<sub>2</sub>O<sub>3</sub> film studied by Auger electron spectroscopy. *Appl Surf Sci* **185**(3-4), 248-254.
- HERNANDEZ, L.S., MIRANDA, J.M., NARVAEZ, L. & DOMINGUEZ, O. (2003). Comparative corrosion behaviour of Zn-21Al-2Cu alloy and galvanized steel. *Corro Prevent Contr* **50**(2), 53-63.
- HUMPHREYS, F.J. (1999). Quantitative metallography by electron backscattered diffraction. *J Microsc (Oxf)* **195**, 170-185.
- NEGRETE, J., TORRES, A., NARVAEZ, L., ZAMORA, J. & TORRES-VILLASENOR, G. (1999). Microstructural changes during hot rolling of the cast Zn-21Al-2Cu alloy. *Revista Mexicana De Fisica* **45**, 134-137.
- NEGRETE, J., TORRES, A. & TORRES-VILLASENOR, G. (1995). Thermal treatments of as-extruded eutectoid Zn-21.2Al-1.9 wt% Cu alloy. *J Mater Sci Lett* **14**(15), 1092-1094.
- NOWELL, M.M., WITT, R.A. & TRUE, B. (2005). EBSD sample preparation: Techniques, tips, and tricks. *Microsc Microanal* **11**(Suppl S02), 504-505.
- RAMOS AZPEITIA, M., MARTINEZ FLORES, E.E. & TORRES VILLASENOR, G. (2012). Superplastic behavior of Zn-Al eutectoid alloy with 2% Cu. *J Mater Sci* **47**(17), 6206-6212.
- SCHWARTZ, A.J., KUMAR, M., ADAMS, B.L. & FIELD, D.P.E. (2009). *Electron Backscatter Diffraction in Materials Science*. New York: Springer.
- TORRES-VILLASENOR, G., UGALDE, A., HERNANDEZ, L. & SINGER, I.L. (1984). Water-Vapor corrosion of lamellar, superplastic and cast dendritic Zn-21Al alloy. *Corros Sci* **24**(3), 4.
- TSL-EDAX (2001). OIM Analysis User Manual. Utah, USA: TexSEM Laboratories Incorporated.
- VANDER VOORT, G.F. (1999). *Metallography: Principles and Practice*. OH, NY: Mc Graw Hill, ASM International, Materials Park.
- VANDER VOORT, G.F. (2011a). Metallographic specimen preparation for electron backscattered diffraction. Part I. *Pract Metallogr* **48**(9), 454-473.
- VANDER VOORT, G.F. (2011b). Metallographic specimen preparation for electron backscattered diffraction. Part II. *Pract Metallogr* **48**(10), 527-543.
- WARYOBA, D. & KALU, P. (2003). Orientation imaging microscopy: Sample preparation for heavily drawn copper wires. *Microsc Microanal* **9**(Suppl S02), 84-85.
- WITT, R. & NOWELL, M. (2011). Specimen preparation of difficult materials for EBSD characterization. *Microsc Microanal* **17**(Suppl S2), 414-415.
- WRIGHT, S.I. & NOWELL, M.M. (2006). EBSD image quality mapping. *Microsc Microanal* **12**(01), 72-84.
- WYNICK, G.L. & BOEHLERT, C.J. (2005). Electron backscattered diffraction characterization technique for analysis of a Ti<sub>2</sub>AlNb intermetallic alloy. *J Microsc (Oxf)* **219**, 115-121.
- ZHU, Y.H., LEE, W.B. & TO, S. (2003). Use of EBSD to study stress induced microstructural changes in Zn-Al based alloy. *Mater Sci Eng A-Struct Mater* **348**(1-2), 6-14.
- ZHU, Y.H., LEE, W.B., YEUNG, C.F. & YUE, T.M. (2001). EBSD of Zn-rich phases in Zn-Al-based alloys. *Mater Charact* **46**(1), 19-23.
- ZIPPERIAN, D. (2011). Final polishing. In *Metallographic Handbook*, PACE Technologies (Ed.), vol. 2, 344pp. Tucson, AZ, USA: Technologies, Pace.